J. Vis. Commun. Image R. 22 (2011) 529–542

Contents lists available at ScienceDirect

J. Vis. Commun. Image R.

journal homepage: www.elsevier.com/locate/jvci

Fast image inpainting and colorization by Chambolle's dual method

Fang Li [a], Zheng Bao [b], Ruihua Liu [c], Guixu Zhang [d,*]

[a] Department of Mathematics, East China Normal University, Shanghai, China
[b] Huaya Microelectronic, Inc., Shanghai, China
[c] School of Mathematics and Statistics, Chongqing University of Technology, Chongqing, China
[d] Department of Computer Science, East China Normal University, Shanghai, China

ARTICLE INFO

Article history:
Received 4 October 2009
Accepted 23 June 2011
Available online 7 July 2011

Keywords:
Inpainting
Colorization
Total variation
Chambolle's dual method

ABSTRACT

In this paper, we propose to use Chambolle's dual methods to solve Total Variation (TV) inpainting model and (weighted) TV colorization model. The fidelity coefficients in these two models are functions which taking zero in the inpainting region and a positive constant in the other region. Then Chambolle's dual method can not be directly used to solve these models since the fidelity coefficient will be denominator in the algorithm. In order to overcome this drawback, we propose to approximate these models by adding new variables. Then the approximated problems can be solved by alternating minimization method with Chambolle's dual method and closed form solutions which is fast and easy to implement. Mathematical results of existence of minimizers are proved for both the original and the approximated problems. Numerical results and comparison with other closely related methods demonstrate that our algorithms are quite efficient.

1. Introduction

Image inpainting is an important topic in computer vision and image processing. The goal is to recover missing data in a damaged image. It is widely used in film restoration, text removal, scratch removal, and special effects in movies. An important class of digital inpainting methods relates to partial differential equations (PDEs). The term of digital inpainting was initially introduced by Bertalmio et al. in [5]. The authors were the first to apply PDEs in image inpainting. In their method, the information outside the inpainting region is propagated into the inpainting region along isophotes driven by a third-order gradient decent flow. Ballester et al. in [3] proposed to smoothly extend inside the inpainting domain both the vector field obtained from the image gradient and the isophotes. Bertalmio et al. in [6] introduced the Navier–Stokes equations for fluid dynamics into image inpainting. Chan et al. in [13] proposed total variation (TV) inpainting algorithm by modifying the Rudin–Osher–Fatemi (ROF) model [29] with fidelity coefficient zero in the inpainting domain and positive constant in the information domain. The inpainting error can be estimated [15]. Then the same authors in [14] proposed a curvature-driven diffusion (CDD) PDE inpainting model which extends the TV algorithm by taking into account geometric information of isophotes (i.e. curvature) in the total variation diffusion equation, thus can connect some broken edges. Masnou et al. in [26] and Chan et al. in [17] studied the variational inpainting models based on Euler elastica in which curvature is also involved. Grossauer et al. in [23] used the complex Ginzburg Landau equation for digital inpainting in 2D and 3D. Tai et al. in [32] proposed to first propagate the isophote directions into the inpainting region by TV-Stokes equation and then the image is restored to fit the constructed directions. These PDE-based image inpainting methods have the advantage of preserving edges very well, however, the slow and unstable numerical implementations greatly limit their practical use. PDE based inpainting techniques are suitable for non-texture image inpainting. Another class of approaches based on texture synthesis is suitable for texture image inpainting, in which exemplar-based method seems very successful [18,28]. This two classes of methods can be combined together [22,7]. Recently wavelet and framelet are used in image inpainting [11,12].

Image colorization is to inpainting color image from a grayscale image with color data given only in small regions. Levin et al. in [25] proposed to minimize a quadratic cost function derived from the color differences between a pixel and its weighted average neighborhood. The solution is found by solving linear system. Sapiro in [30] proposed to minimize the difference between the gradient of luminance and the gradient of color which results in solving Poisson equations. Yatziv et al. in [34] proposed a fast image and video colorization method using chrominance blending with Dijkstra's shortest path algorithm. Kang et al. in [24] extended TV inpainting method to TV colorization. The main difference of TV inpainting and TV colorization is that the latter has a constraint, that is, the chrominance takes value on the sphere. The authors also proposed a weighted harmonic model for image colorization.

* Corresponding author.
E-mail address: gxzhang@cs.ecnu.edu.cn (G. Zhang).

1047-3203/$ - see front matter © 2011 Elsevier Inc. All rights reserved.
doi:10.1016/j.jvcir.2011.06.006

In this paper, we take use of Chambolle's dual method to solve TV inpainting and TV colorization model. Chambolle's dual method is called dual method for simplicity in this paper. This dual method has important advantages: firstly, it minimizes the exact TV norm unlike usual approaches; secondly, it is fast and easy to implement. This dual method is originally designed to solve the ROF model with positive constant fidelity coefficient, and it cannot be directly used in solving neither TV inpainting nor TV colorization. In [8,9], the technique of adding new variable is widely used to approximate some variational denoising and segmentation functionals such that the approximate problems can be solved efficiently by Chambolle's dual method. We follow their idea in this paper. We approximate the TV inpainting and TV colorization model by adding new variables, and then the approximate energies can be minimized by dual method and closed form solutions. Especially, we use Lagrange multipliers method to handle the constraint in TV colorization, which leads to a closed form solution of multipliers.

The outline of this paper is as follows. In Section 2, we propose our methods to solve TV inpainting problem for gray scale image and color image respectively. Some meaningful mathematical results are proved. In Section 3, we study the weighted TV colorization model and the existence of minimizer. We give the numerical results of our algorithms in Section 4. We also compare our approach with the most related methods. Finally, we conclude the paper in Section 5.

2. TV inpainting with dual method

2.1. The model

For mathematical modeling, we review some properties of bounded variation (BV) space. Assume $\Omega \subset \mathbb{R}^2$ is the bounded domain with Lipschitz boundary. The bounded variation space $BV(\Omega)$ is a subspace of functions $u \in L^1(\Omega)$ such that the following quantity is finite

$$\int_\Omega |\nabla u| dx := \sup\left\{ \int_\Omega u \mathrm{div}\boldsymbol{\varphi} dx \mid \boldsymbol{\varphi} \in C_c^1(\Omega, \mathbb{R}^2), |\boldsymbol{\varphi}| \leqslant 1 \right\}$$

$BV(\Omega)$ endowed with the norm $\|u\|_{BV} = \int_\Omega |\nabla u| dx + \|u\|_{L^1(\Omega)}$ is a Banach space. The term $\int_\Omega |\nabla u| dx$ is called the total variation of u. Here ∇u is understood as a Radon measure. BV space is widely used in variational image modeling [2]. It has the following compactness property in BV-w* topology: If $\{u^n\}$ is a uniformly bounded sequence in $BV(\Omega)$, then up to a subsequence, there exists a function $u \in BV(\Omega)$ such that $u_n \rightharpoonup u$ weakly* in $BV(\Omega)$ (i.e., $\nabla u_n \rightharpoonup \nabla u$ weakly* in the sense of measure) and $u_n \to u$ strongly in $L^1(\Omega)$. See [2,20] for more details.

The definition is generalized to vectorial functions. We define the space $BV(\Omega, \mathbb{R}^3)$ of vector valued functions as the set of functions $\mathbf{u} \in L^1(\Omega, \mathbb{R}^3)$ such that the vectorial TV norm

$$\int_\Omega |\nabla \mathbf{u}| dx := \sup\left\{ \int_\Omega \sum_{i=1}^{3} u_i \mathrm{div}\mathbf{q}_i dx \mid \mathbf{q} \in C_c^1(\Omega, \mathbb{R}^{3\times 2}), |\mathbf{q}| \leqslant 1 \right\},$$

where $|\mathbf{q}| = \sqrt{|\mathbf{q}_1|^2 + |\mathbf{q}_2|^2 + |\mathbf{q}_3|^2}$. $BV(\Omega, \mathbb{R}^3)$ endowed with the norm $\|\mathbf{u}\|_{BV(\Omega,\mathbb{R}^3)} = \int_\Omega |\nabla \mathbf{u}| dx + \|\mathbf{u}\|_{L^1(\Omega,\mathbb{R}^3)}$ is a Banach space. Standard results such as lower semi-continuous and compactness property hold for vectorial BV functions [9].

In the following, we propose our approximate models of TV inpainting for gray scale image and color image respectively.

2.1.1. Gray scale image inpainting

Assume $\Omega \subset \mathbb{R}^2$ is the bounded image domain with Lipschitz boundary and $f : \Omega \to \mathbb{R}$ is the gray scale image. Let $D \subset \Omega$ be the inpainting domain and $D^c = \Omega \backslash D$ be the complement of D in Ω. The TV inpainting model proposed in [13] is a modified ROF model as

$$\min_{u\in BV(\Omega)} E(u) = \int_\Omega |\nabla u| dx + \frac{\lambda}{2}\int_{D^c} (u-f)^2 dx$$

with $\lambda > 0$ is a constant, or equivalently,

$$\min_{u\in BV(\Omega)} E(u) = \int_\Omega |\nabla u| dx + \frac{1}{2}\int_\Omega \hat{\lambda}(u-f)^2 dx, \tag{1}$$

where

$$\hat{\lambda} = \begin{cases} \lambda, & x \in D^c \\ 0, & x \in D \end{cases}$$

Though many fast algorithms have been proposed to solve the ROF restoration model, most of them can not be directly used to solve problem (1) since $\hat{\lambda}$ takes value zero in D. For example, considering Chambolle's dual algorithm in [10], the following formula will be involved:

$$u = f - \frac{1}{\hat{\lambda}}\mathrm{div}\mathbf{p}.$$

The algorithm of Nesterov [27] also includes the similar formula and can not be used directly. The FISTA algorithm in [4] also involves the factor $1/\hat{\lambda}$. This difficulty can not be overcome by projection operator as algorithm I in [11]. In that algorithm, the inpainting and denoising are split into two steps in fact, then it is not really solving problem (1) exactly. While the split Bregman (SB) algorithm proposed in [21] can be directly used to solve problem (1). The SB algorithm is shown to be very fast in image denoising and is one of the state of the art. The SB algorithm is closely related to many other algorithms [19,31].

In this paper, we propose another method to overcome this difficulty. We add an auxiliary variable v and minimize

$$E_\theta(u, v) = \int_\Omega |\nabla v| dx + \frac{1}{2\theta}\int_\Omega (u-v)^2 dx + \frac{1}{2}\int_\Omega \hat{\lambda}(u-f)^2 dx, \tag{2}$$

where θ is small enough such that v approximates u in the sense of L^2 norm.

2.1.2. Color image inpainting

Let $\mathbf{f} : \Omega \to \mathbb{R}^3$ be a color image. Following the same line as the gray image case, we can easily extend the TV inpainting model for gray scale image to color image inpainting. The energy functional is

$$E(\mathbf{u}) = \int_\Omega |\nabla \mathbf{u}| dx + \frac{1}{2}\int_\Omega \hat{\lambda}(\mathbf{u}-\mathbf{f})^2 dx. \tag{3}$$

By adding auxiliary variable $\mathbf{v}$, the above energy can be approximated by

$$E_\theta(\mathbf{u}, \mathbf{v}) = \int_\Omega |\nabla \mathbf{v}| dx + \frac{1}{2\theta}\int_\Omega (\mathbf{u}-\mathbf{v})^2 dx + \frac{1}{2}\int_\Omega \hat{\lambda}(\mathbf{u}-\mathbf{f})^2 dx, \tag{4}$$

where θ is small enough such that $\mathbf{v}$ approximates $\mathbf{u}$ in the sense of L^2 norm.

2.2. Mathematical analysis

First we consider the existence of minimizer to TV inpainting model (1) for gray scale image. Remark that Chan et al. [17] proved the existence of minimizer for a constrained TV inpainting model where the constraint ($u \in [0,1]$) simplifies the proof but is not natural. In this paper, we will consider the original TV inpainting problem. However, the problem is hard to handle directly. Let us consider a minimizing sequence $\{u_n\} \in BV(\Omega)$ for problem (1). Then $E(u_n)$ is bounded, i.e., there exists a constant C such that

$$\int_\Omega |\nabla u_n| dx + \frac{1}{2}\int_\Omega \hat{\lambda}(u_n - f)^2 dx \leqslant C.$$

Then we can deduce that $\int_\Omega |\nabla u_n| dx$ is uniformly bounded. Unfortunately we cannot deduce that u_n is uniformly bounded in $L^1(\Omega)$. So we need to consider a regularized version of $E(u)$, that is, we consider the following approximate problem

$$\min_{u\in H^1(\Omega)} E_\epsilon(u) = \int_\Omega |\nabla u| dx + \frac{1}{2}\int_\Omega \hat{\lambda}(u-f)^2 dx + \frac{\epsilon}{2}\int_\Omega (u^2 + |\nabla u|^2) dx. \tag{5}$$

We first prove the existence and uniqueness of minimizer to problem (5). Then we prove that a maximum principle holds for a solution of (5). After that we get back to the original problem (1) by letting $\epsilon \to 0^+$ in (5).

Proposition 1. *For fixed $\epsilon > 0$, problem (5) has a unique minimizer $u_\epsilon \in H^1(\Omega)$.*

Proof. Since the functional (5) is strictly convex, lower semi-continuous and coercive over the Hilbert space $H^1(\Omega)$, we can get the existence and the uniqueness of minimizer by a standard argument. □

By standard variational methods, we can derive the Euler-Lagrange equation of problem (5).

Proposition 2. *Assume u_ϵ is the solution of problem (5), then u_ϵ satisfies the Euler–Lagrange equation*

$$-\mathrm{div}\left(\frac{\nabla u_\epsilon}{|\nabla u_\epsilon|}\right) + \hat{\lambda}(u_\epsilon - f) + \epsilon u_\epsilon - \epsilon \triangle u_\epsilon = 0 \tag{6}$$

in the distribution sense. Moreover, u_ϵ satisfies Neumann conditions $\frac{\partial u_\epsilon}{\partial N} = 0$ on the boundary $\partial\Omega$.

Note that in this paper $-\mathrm{div}\left(\frac{\nabla u_\epsilon}{|\nabla u_\epsilon|}\right)$ is understood as the subdifference of the total variation of u_ϵ. See [1] for more details.

Let us now show that u_ϵ satisfies a maximum principle.

Proposition 3. *Assume $f \in L^\infty(\Omega)$ and u_ϵ is the solution of problem (5). Then*

$$\operatorname{ess\,inf}_\Omega f \leqslant u_\epsilon \leqslant \operatorname{ess\,sup}_\Omega f.$$

Proof. We first multiply Eq. (6) by a function $v \in H^1(\Omega)$, and integrate by parts:

$$\int_\Omega \left(\frac{\nabla u_\epsilon}{|\nabla u_\epsilon|}\right)\nabla v dx + \hat{\lambda}\int_\Omega (u_\epsilon - f) v dx + \epsilon\int_\Omega u_\epsilon v + \epsilon\int_\Omega \nabla u_\epsilon \cdot \nabla v dx = 0, \tag{7}$$

where the Neumann boundary condition is used. Let G be a truncation function of class C^1, such that $G(t) = 0$ on $(-\infty, 0]$, and G strictly increasing on $[0, +\infty)$, and $G' \leqslant M$ where M is a constant. We choose $v = G(u_\epsilon - k)$ where k is a constant such that $k \geqslant \|f\|_\infty$. Thanks to the chain rule in $H^1(\Omega)$, $v = G(u_\epsilon - k)$ also belongs to $H^1(\Omega)$, and $\nabla v = G'(u_\epsilon - k)\nabla u_\epsilon$. Then Eq. (7) can be rewritten as

$$\int_\Omega |\nabla u_\epsilon| G'(u_\epsilon - k) dx + \hat{\lambda}\int_\Omega (u_\epsilon - f) G(u_\epsilon - k) dx + \epsilon\int_\Omega u_\epsilon G(u_\epsilon - k) dx + \epsilon\int_\Omega |\nabla u_\epsilon|^2 G'(u_\epsilon - k) dx = 0.$$

Using the properties of G, we deduce that

$$\hat{\lambda}\int_\Omega (u_\epsilon - f) G(u_\epsilon - k) dx + \epsilon\int_\Omega u_\epsilon G(u_\epsilon - k) dx \leqslant 0.$$

Then

$$\hat{\lambda}\int_\Omega (u_\epsilon - k + k - f) G(u_\epsilon - k) dx + \epsilon\int_\Omega (u_\epsilon - k + k) G(u_\epsilon - k) dx \leqslant 0.$$

Since $k - f \geqslant 0$, we have

$$(\hat{\lambda} + \epsilon)\int_\Omega (u_\epsilon - k) G(u_\epsilon - k) dx \leqslant 0$$

which implies $u_\epsilon \leqslant k$. Since this last inequality holds for any k such that $k \geqslant \|f\|_\infty$, we obtain that $u_\epsilon \leqslant \operatorname{ess\,sup}_\Omega f$. Similarly, we can prove $\operatorname{ess\,inf}_\Omega f \leqslant u_\epsilon$. □

Now we can pass to the limit $\epsilon \to 0^+$ in (5).

Theorem 1. *Let f be in $L^\infty(\Omega)$, then problem (1) has at least one solution u in $BV(\Omega)$ satisfying*

$$\operatorname{ess\,inf}_\Omega f \leqslant u \leqslant \operatorname{ess\,sup}_\Omega f.$$

Proof. We already know that

$$\operatorname{ess\,inf}_\Omega f \leqslant u_\epsilon \leqslant \operatorname{ess\,sup}_\Omega f \tag{8}$$

which means u_ϵ is uniformly bounded in $L^2(\Omega)$. Meanwhile, since u_ϵ is a solution of problem (5), we have $E_\epsilon(u_\epsilon) \leqslant E_\epsilon(v)$ for all v in $H^1(\Omega)$, i.e.,

$$\begin{aligned} E_\epsilon(u_\epsilon) &= \int_\Omega |\nabla u_\epsilon| dx + \frac{1}{2}\int_\Omega \hat{\lambda}(u_\epsilon - f)^2 dx + \frac{\epsilon}{2}\int_\Omega (u_\epsilon^2 + |\nabla u_\epsilon|^2) dx \\ &\leqslant \int_\Omega |\nabla v| dx + \frac{1}{2}\int_\Omega \hat{\lambda}(v-f)^2 dx + \frac{\epsilon}{2}\int_\Omega (v^2 + |\nabla v|^2) dx \\ &= E_\epsilon(v). \end{aligned}$$

If we take $v \equiv 0$, it holds that

$$\int_\Omega |\nabla u_\epsilon| dx \leqslant \frac{1}{2}\int_\Omega \hat{\lambda} f^2 dx.$$

We conclude that u_ϵ is uniformly bounded in $BV(\Omega) \cap L^2(\Omega)$ uniformly in ϵ. Consider a sequence ϵ^n such that $\epsilon^n > 0$ and $\epsilon^n \to 0$ as $n \to \infty$. There exists u in $BV(\Omega) \cap L^2(\Omega)$ such that up to a subsequence,

$$u_{\epsilon^n} \rightharpoonup u \text{ weakly}^* \text{ in } BV(\Omega),$$

$$u_{\epsilon^n} \to u \text{ strongly in } L^1(\Omega),$$

$$u_{\epsilon^n} \rightharpoonup u \text{ weakly in } L^2(\Omega).$$

From (8), we have $\operatorname{ess\,inf}_\Omega f \leqslant u \leqslant \operatorname{ess\,sup}_\Omega f$,and thanks to the lower semi-continuity of total variation and L^2 norm, we obtain for all $v \in H^1(\Omega)$ that

$$\begin{aligned} E(u) &= \int_\Omega |\nabla u| dx + \frac{1}{2}\int_\Omega \hat{\lambda}(u-f)^2 dx \leqslant \liminf_{\epsilon\to 0^+} \int_\Omega |\nabla u_\epsilon| dx \\ &\quad + \frac{1}{2}\int_\Omega \hat{\lambda}(u_\epsilon - f)^2 dx \\ &= \liminf_{\epsilon\to 0^+} \int_\Omega |\nabla u_\epsilon| dx + \frac{1}{2}\int_\Omega \hat{\lambda}(u_\epsilon - f)^2 dx \\ &\quad + \frac{\epsilon}{2}\int_\Omega (u_\epsilon^2 + |\nabla u_\epsilon|^2) dx = \liminf_{\epsilon\to 0^+} E_\epsilon(u_\epsilon) \leqslant \lim_{\epsilon\to 0^+} E_\epsilon(v) \\ &= \int_\Omega |\nabla v| dx + \frac{1}{2}\int_\Omega \hat{\lambda}(v-f)^2 dx = E(v). \end{aligned} \tag{9}$$

Since the function $u \in BV(\Omega) \cap L^2(\Omega)$ can be approximated by a sequence of functions in $H^1(\Omega)$ (see [20], Section 5.2.2, Theorem 2), we get that (9) holds for any $v \in BV(\Omega)$, i.e., u is a minimizer of E. □

Now we consider the existence of minimizer for the approximate problem (2). This problem is hard to handle directly too. Hence we first construct an approximate problem as

$$\min_{(u,v)\in L^2(\Omega)\times H^1(\Omega)} E_\theta^\epsilon(u,v) = \int_\Omega |\nabla v|dx + \frac{1}{2\theta}\int_\Omega (u-v)^2dx + \frac{1}{2}\int_\Omega \hat{\lambda}(u-f)^2dx + \frac{\epsilon}{2}\int_\Omega (v^2+|\nabla v|^2)dx. \quad (10)$$

With similar argument as above, we can prove the following results. For simplicity, we state them without proof.

Proposition 4. *For fixed $\epsilon > 0$, $\theta > 0$, problem (10) has a unique minimizer $(u_\theta^\epsilon, v_\theta^\epsilon) \in L^2(\Omega)\times H^1(\Omega)$.*

Proposition 5. *Assume $(u_\theta^\epsilon, v_\theta^\epsilon)$ is the solution of problem (10), then $(u_\theta^\epsilon, v_\theta^\epsilon)$ satisfies the Euler-Lagrange equations*

$$-\operatorname{div}\left(\frac{\nabla v_\theta^\epsilon}{|\nabla v_\theta^\epsilon|}\right) + \frac{1}{\theta}(v_\theta^\epsilon - u_\theta^\epsilon) + \epsilon v_\theta^\epsilon - \epsilon\triangle v_\theta^\epsilon = 0, \quad (11)$$

$$u_\theta^\epsilon = \frac{\hat{\lambda}\theta f + v_\theta^\epsilon}{1+\hat{\lambda}\theta} \quad (12)$$

in the distribution sense. Moreover, v_θ^ϵ satisfies Neumann conditions $\frac{\partial v_\theta^\epsilon}{\partial N} = 0$ on the boundary $\partial\Omega$.

Proposition 6. *Assume $f \in L^\infty(\Omega)$ and $(u_\theta^\epsilon, v_\theta^\epsilon)$ is the solution of problem (10). Then*

$$\operatorname{ess\,inf}_\Omega f \leqslant v_\theta^\epsilon \leqslant \operatorname{ess\,sup}_\Omega f.$$

Theorem 2. *Let f be in $L^\infty(\Omega)$ and fix $\theta > 0$, then problem (2) has at least one solution (u_θ, v_θ) in $L^2(\Omega)\times BV(\Omega)$ satisfying*

$$\operatorname{ess\,inf}_\Omega f \leqslant v_\theta \leqslant \operatorname{ess\,sup}_\Omega f. \quad (13)$$

Finally we pass the limit as $\theta \to 0^+$ and establish the relationship of solutions to the approximate problem (2) and the original problem (1).

Theorem 3. *As $\theta \to 0^+$, the solution of the approximate problem (2) converges to the solution of the original problem (1).*

Proof. Assume (u_θ, v_θ) is a solution of problem (2) for fixed $\theta \in (0,1)$, we have $E_\theta(u_\theta, v_\theta) \leqslant E_\theta(w,\varphi)$ for all $(w,\varphi) \in L^2(\Omega)\times BV(\Omega)$, i.e.,

$$\int_\Omega |\nabla v_\theta|dx + \frac{1}{2\theta}\int_\Omega (u_\theta - v_\theta)^2dx + \frac{1}{2}\int_\Omega \hat{\lambda}(u_\theta - f)^2dx \leqslant \int_\Omega |\nabla\varphi|dx + \frac{1}{2\theta}\int_\Omega (w-\varphi)^2dx + \frac{1}{2}\int_\Omega \hat{\lambda}(w-f)^2dx.$$

Let $(w,\varphi) \equiv (0,0)$, we obtain

$$\int_\Omega |\nabla v_\theta|dx + \frac{1}{2\theta}\int_\Omega (u_\theta - v_\theta)^2dx + \frac{1}{2}\int_\Omega \hat{\lambda}(u_\theta - f)^2dx \leqslant \frac{1}{2}\int_\Omega \hat{\lambda}f^2dx.$$

Then there exists a constant M such that

$$\int_\Omega |\nabla v_\theta|dx \leqslant M,$$
$$\tfrac{1}{2}\int_\Omega (u_\theta - v_\theta)^2dx \leqslant M\theta \leqslant M.$$

Together with the inequality (13), we conclude that u_θ is uniformly bounded in $L^2(\Omega)$ and v_θ is uniformly bounded in $BV(\Omega)\cap L^2(\Omega)$ uniformly in ϵ. Consider a sequence θ^n such that $\theta^n > 0$ and $\theta^n \to 0$ as $n \to \infty$. There exists $(u,v) \in L^2(\Omega)\cap BV(\Omega)$ such that up to a subsequence,

$$u_{\theta^n} \rightharpoonup u \text{ weakly in } L^2(\Omega),$$
$$v_{\theta^n} \rightharpoonup v \text{ weakly}^* \text{ in } BV(\Omega),$$
$$v_{\theta^n} \to v \text{ strongly in } L^1(\Omega),$$
$$v_{\theta^n} \rightharpoonup v \text{ weakly in } L^2(\Omega),$$
$$u_{\theta^n} - v_{\theta^n} \to 0 \text{ strongly in } L^2(\Omega).$$

Hence $u = v$ a.e. $x \in \Omega$. Thanks to the lower semi-continuity of total variation and L^2 norm, we obtain for all $w \in BV(\Omega)$ that

$$\begin{aligned} E(u) &= \int_\Omega |\nabla u|dx + \frac{1}{2}\int_\Omega \hat{\lambda}(u-f)^2dx \\ &\leqslant \liminf_{n\to\infty}\int_\Omega |\nabla v_{\theta^n}|dx + \frac{1}{2\theta^n}\int_\Omega (u_{\theta^n} - v_{\theta^n})^2dx + \frac{1}{2}\int_\Omega \hat{\lambda}(u_{\theta^n} - f)^2dx \\ &= \liminf_{n\to\infty} E_{\theta^n}(u_{\theta^n}, v_{\theta^n}) \leqslant \liminf_{n\to\infty} E_{\theta^n}(w,w) \\ &= \int_\Omega |\nabla w|dx + \frac{1}{2}\int_\Omega \hat{\lambda}(w-f)^2dx = E(w). \end{aligned}$$

Thus u is a minimizer of E. □

Remark 1. Since the TV inpainting functional E in (1) and the approximate funtional E_θ in (2) are not strictly convex, uniqueness of minimizers are not guaranteed. Nonuniqueness of minimizers for the TV inpainting model is also discussed in [17]. See for example the Fig. 4.1 in [17]. The above mathematical analysis and results can be trivially extended to color TV inpainting model (3) and its approximate problem (4), thus is omitted.

2.3. The algorithm

For gray scale image inpainting, the approximate problem (2) can be solved by alternating minimization methods. We solve the following two subproblems iteratively,

$$\min_v \int_\Omega |\nabla v|dx + \frac{1}{2\theta}\int_\Omega (u-v)^2dx, \quad (14)$$

$$\min_u \frac{1}{2\theta}\int_\Omega (u-v)^2dx + \frac{1}{2}\int_\Omega \hat{\lambda}(u-f)^2dx. \quad (15)$$

Problem (14) can be solved by Chambolle's dual method. The solution is given by

$$v = u - \theta\operatorname{div}\mathbf{p}^*, \quad (16)$$

where the vector $\mathbf{p}^*$ can be solved by fixed point method: Initializing $\mathbf{p}^0 = \mathbf{0}$ and iterating

$$\mathbf{p}^{n+1} = \frac{\mathbf{p}^n + \tau\nabla(\operatorname{div}\mathbf{p}^n - u/\theta)}{1+\tau|\nabla(\operatorname{div}\mathbf{p}^n - u/\theta)|} \quad (17)$$

with $\tau \leqslant 1/8$ to ensure the convergence. See [10] for more details. Problem (15) has closed form solution, i.e.,

$$u = \frac{\hat{\lambda}\theta f + v}{1+\hat{\lambda}\theta}.$$

Remark that in our implementation, we slightly modified the dual method. In the alternative minimization process, one iteration is needed to solve $\mathbf{p}^*$ with initial $\mathbf{p}$ in the last loop. The algorithm details are as follows.

2.4. Algorithm I

- Initialization: $u^0 = f$, $\mathbf{p}^0 = \mathbf{0}$.
- Iteration: for $k = 0, 1, 2, \ldots$

$$\mathbf{p}^{k+1} = \frac{\mathbf{p}^k + \tau\nabla(\mathrm{div}\mathbf{p}^k - u^k/\theta)}{1 + \tau\left|\nabla(\mathrm{div}\mathbf{p}^k - u^k/\theta)\right|},$$

$$v^{k+1} = u^k - \theta\mathrm{div}\mathbf{p}^{k+1},$$

$$u^{k+1} = \frac{\hat{\lambda}\theta f + v^{k+1}}{1 + \hat{\lambda}\theta}.$$

- Termination criterion: $k > k_{\max}$ where $k_{\max}$ is the maximum iteration defined by the user.

For color image inpainting, the approximated problem can be solved by alternatively solving the following two subproblems

$$\min_{\mathbf{v}} \int_\Omega |\nabla\mathbf{v}|dx + \frac{1}{2\theta}\int_\Omega (\mathbf{u} - \mathbf{v})^2 dx, \tag{18}$$

$$\min_{\mathbf{u}} \frac{1}{2\theta}\int_\Omega (\mathbf{u} - \mathbf{v})^2 dx + \frac{1}{2}\int_\Omega \hat{\lambda}(\mathbf{u} - \mathbf{f})^2 dx. \tag{19}$$

Problem (18) can be solved by Chambolle's dual method which is extended to color image by Bresson et al. in [9]. The solution is given by

$$\mathbf{v} = \mathbf{u} - \theta\mathrm{div}\mathbf{p}^*, \tag{20}$$

where the vector $\mathbf{p}^*$ can be solved by fixed point method: Initializing $\mathbf{p}^0 = \mathbf{0}$ and iterating

$$\mathbf{p}^{n+1} = \frac{\mathbf{p}^n + \tau\nabla(\mathrm{div}\mathbf{p}^n - \mathbf{u}/\theta)}{1 + \tau|\nabla(\mathrm{div}\mathbf{p}^n - \mathbf{u}/\theta)|} \tag{21}$$

which means for each channel $i = 1, 2, 3$

$$\mathbf{p}_i^{n+1} = \frac{\mathbf{p}_i^n + \tau\nabla(\mathrm{div}\mathbf{p}_i^n - \mathbf{u}_i/\theta)}{1 + \tau\sqrt{\sum_{i=1}^3 \left|\nabla(\mathrm{div}\mathbf{p}_i^n - \mathbf{u}_i/\theta)\right|^2}}. \tag{22}$$

Similar to gray image case, the algorithm details are as follows.

2.5. Algorithm II

- Initialization: $\mathbf{u}^0 = \mathbf{f}$, $\mathbf{p}^0 = \mathbf{0}$.
- Iteration: for $k = 0, 1, 2, \cdots$

$$\mathbf{p}^{k+1} = \frac{\mathbf{p}^k + \tau\nabla(\mathrm{div}\mathbf{p}^k - \mathbf{u}^k/\theta)}{1 + \tau\left|\nabla(\mathrm{div}\mathbf{p}^k - \mathbf{u}^k/\theta)\right|},$$

$$\mathbf{v}^{k+1} = \mathbf{u}^k - \theta\mathrm{div}\mathbf{p}^{k+1},$$

$$\mathbf{u}^{k+1} = \frac{\hat{\lambda}\theta\mathbf{f} + \mathbf{v}^{k+1}}{1 + \hat{\lambda}\theta}.$$

- Termination criterion: as Algorithm I.

3. TV colorization with dual method

3.1. The model

Decompose the color image $\mathbf{f} = (\mathbf{f}_1, \mathbf{f}_2, \mathbf{f}_3)$ into two components of chromaticity component $\mathbf{C}_0$ and brightness B_0 as follows:

$$B_0 = |\mathbf{f}| = \sqrt{\mathbf{f}_1^2 + \mathbf{f}_2^2 + \mathbf{f}_3^2}, \quad \mathbf{C}_0 = \frac{\mathbf{f}}{B_0}.$$

Then the chromaticity is a vector on the unit sphere in $\mathbb{R}^3$: $\mathscr{S}^2 = \{\xi \in \mathbb{R}^3 : |\xi| = 1\}$. This Chromaticity-Brightness (CB) model is widely used in color image representation and modeling [16].

Assume the chromaticity $\mathbf{C}_0$ is known in D^c and the brightness B_0 is known everywhere in Ω. Then the colorization problem is to recover the chromaticity in D. Kang et al. in [24] proposed two models for image colorization. One is the TV colorization model:

$$\min_{\mathbf{C}\in BV(\Omega,\mathbb{R}^3),|\mathbf{C}|=1} \int_\Omega |\nabla\mathbf{C}|dx + \frac{1}{2}\int_\Omega \hat{\lambda}|\mathbf{C} - \mathbf{C}_0|^2 dx. \tag{23}$$

The other is via weighted harmonic map:

$$\min_{\mathbf{C}\in W^{1,2}(\Omega,\mathbb{R}^3),|\mathbf{C}|=1} \int_\Omega g|\nabla\mathbf{C}|^2 dx + \frac{1}{2}\int_\Omega \hat{\lambda}|\mathbf{C} - \mathbf{C}_0|^2 dx, \tag{24}$$

where $g = \frac{1}{1 + k|\nabla G_\sigma * B_0|^2}$, G_σ is Gaussian filter with parameter $\sigma > 0$ and $k > 0$ is a constant parameter. The main difficulty in solving these two models lies in how to deal with the constraint $|\mathbf{C}| = 1$. In [24], the constrained problem (24) is transformed into another constrained problem as

$$\min_{\mathbf{C}\in W^{1,2}(\Omega,\mathbb{R}^3),|\mathbf{C}|\leqslant 1} \int_\Omega g|\nabla\mathbf{C}|^2 dx + \frac{1}{2}\int_\Omega \hat{\lambda}|\mathbf{C} - \mathbf{C}_0|^2 dx + \alpha\int_\Omega (|\mathbf{C}| - 1)^2 dx, \tag{25}$$

where α is a positive constant. Then problem (25) is solved by the gradient descent method

$$\mathbf{C}_t = \mathrm{div}(g\nabla\mathbf{C}) - \hat{\lambda}(\mathbf{C} - \mathbf{C}_0) - \alpha\left(1 - \frac{1}{|\mathbf{C}|}\right).$$

Meanwhile, $\mathbf{C}$ is projected to satisfy $|\mathbf{C}| \leqslant 1$ in each iteration. The constraint in problem (23) is handled similar to (24) and then an implicit scheme is used in the algorithm. In our implementation, we find that the second model (24) is more effective and efficient than model (23). Bresson et al. in [9] extended the ROF model to denoise the chromaticity component in color image:

$$\min_{\mathbf{C}\in BV(\Omega,\mathbb{R}^3)} \int_\Omega |\nabla\mathbf{C}|dx + \frac{\lambda}{2}\int_\Omega |\mathbf{C} - \mathbf{C}_0|^2 dx + \alpha\int_\Omega (|\mathbf{C}| - 1)^2 dx, \tag{26}$$

where $\lambda > 0$ on the entire image. Dual method is extended to solve this problem. However, this dual method can not be directly used in the colorization problem since $\hat{\lambda} = 0$ in the inpainting domain D. Notice that other method is proposed to handle the S^2 constraint in [33].

In this paper, we consider the following weighted TV colorization model

$$\min_{\mathbf{C}\in BV(\Omega,\mathbb{R}^3),|\mathbf{C}|=1} F(\mathbf{C}) = \int_\Omega g|\nabla\mathbf{C}|dx + \frac{1}{2}\int_\Omega \hat{\lambda}|\mathbf{C} - \mathbf{C}_0|^2 dx. \tag{27}$$

In order to make use of the dual method, we add an auxiliary variable $\mathbf{U}$ and approximate the above model by

$$\min_{\mathbf{C}\in BV(\Omega,\mathbb{R}^3),|\mathbf{C}|=1} F_\theta(\mathbf{U}, \mathbf{C}) = \int_\Omega g|\nabla\mathbf{U}|dx + \frac{1}{2\theta}\int_\Omega |\mathbf{U} - \mathbf{C}|^2 dx + \frac{1}{2}\int_\Omega \hat{\lambda}|\mathbf{C} - \mathbf{C}_0|^2 dx, \tag{28}$$

where θ is small enough.

3.2. Mathematical analysis

We first prove the existence of minimizer to the weighted TV colorization model (27). Then we prove the existence of minimizer to the approximate model (28). Finally we can prove that the solution of the approximate model (28) converges to the solution of the original problem (27) as $\theta \to 0^+$.

It is natural to assume B_0 is in $L^\infty(\Omega)$. Since G_σ is a mollifier, it is easy to see that

$$g = \frac{1}{1 + k|\nabla G_\sigma * B_0|^2} \geqslant \frac{1}{1 + k\|B_0\|_\infty}. \tag{29}$$

Theorem 4. *There exists a minimizer $\mathbf{C} \in BV(\Omega, \mathbb{R}^3)$ of problem (27) satisfying $|\mathbf{C}| = 1$.*

Proof. Assume $\{\mathbf{C}_n \in BV(\Omega, \mathbb{R}^3), |\mathbf{C}_n| = 1\}$ is a minimizing sequence of problem (27) such that

$$\lim_{n\to\infty} F(\mathbf{C}_n) = \inf_{\mathbf{C}} F(\mathbf{C}).$$

Then there exists a constant $M > 0$ such that

$$F(\mathbf{C}_n) = \int_\Omega g|\nabla \mathbf{C}_n|dx + \frac{1}{2}\int_\Omega \hat{\lambda}|\mathbf{C}_n - \mathbf{C}_0|^2 dx \leqslant M.$$

Thanks to g is bounded below by a positive constant in (29) and $\hat{\lambda} \geqslant 0$, we deduce that

$$\int_\Omega |\nabla \mathbf{C}_n| dx \leqslant M.$$

Together with $|\mathbf{C}_n| = 1$, we conclude that $\{\mathbf{C}_n\}$ is uniformly bounded in $BV(\Omega, \mathbb{R}^3) \cap L^2(\Omega, \mathbb{R}^3)$. Then there exists a subsequence, also denoted as $\{\mathbf{C}_n\}$, and a function $\mathbf{C} \in BV(\Omega, \mathbb{R}^3) \cap L^2(\Omega, \mathbb{R}^3)$ such that

$\mathbf{C}_n \rightharpoonup \mathbf{C}$ weakly* in $BV(\Omega, \mathbb{R}^3)$,
$\mathbf{C}_n \to \mathbf{C}$ strongly in $L^1(\Omega, \mathbb{R}^3)$,
$\mathbf{C}_n \rightharpoonup \mathbf{C}$ weakly in $L^2(\Omega, \mathbb{R}^3)$,
$\mathbf{C}_n \to \mathbf{C}$ *a.e.* $x \in \Omega$.

Thus $|\mathbf{C}| = 1$ a.e. $x \in \Omega$. By the lower semi-continuity of weighted total variation and L^2 norm, we obtain

$$\begin{aligned}&\int_\Omega g|\nabla \mathbf{C}|dx + \frac{1}{2}\int_\Omega \hat{\lambda}|\mathbf{C} - \mathbf{C}_0|^2 dx \\ &\quad\leqslant \liminf_{n\to\infty} \int_\Omega g|\nabla \mathbf{C}_n|dx + \frac{1}{2}\int_\Omega \hat{\lambda}|\mathbf{C}_n - \mathbf{C}_0|^2 dx.\end{aligned}$$

That is

$$F(\mathbf{C}) \leqslant \liminf_{n\to\infty} F(\mathbf{C}_n) = \inf_{\mathbf{C}} F(\mathbf{C}).$$

This proves that $\mathbf{C}$ is a minimizer of problem (27) satisfying $|\mathbf{C}| = 1$. □

Theorem 5. *For fixed $\theta > 0$, there exists a minimizer $(\mathbf{U}_\theta, \mathbf{C}_\theta) \in BV(\Omega, \mathbb{R}^3) \times L^2(\Omega, \mathbb{R}^3)$ of the approximate problem (28) satisfying $|\mathbf{C}_\theta| = 1$.*

Proof. Assume $(\mathbf{U}_\theta^n, \mathbf{C}_\theta^n)$ is a minimizing sequence satisfying $|\mathbf{C}_\theta^n| = 1$. There exists a constant $M > 0$ such that

$$\begin{aligned}F_\theta(\mathbf{U}_\theta^n, \mathbf{C}_\theta^n) &= \int_\Omega g|\nabla \mathbf{U}_\theta^n|dx + \frac{1}{2\theta}\int_\Omega |\mathbf{U}_\theta^n - \mathbf{C}_\theta^n|^2 dx \\ &\quad + \frac{1}{2}\int_\Omega \hat{\lambda}|\mathbf{C}_\theta^n - \mathbf{C}_0|^2 dx \leqslant M.\end{aligned}$$

Then

$$\int_\Omega g|\nabla \mathbf{U}_\theta^n|dx \leqslant M,$$
$$\tfrac{1}{2\theta}\int_\Omega |\mathbf{U}_\theta^n - \mathbf{C}_\theta^n|^2 dx \leqslant M. \qquad \square$$

Thanks to g is bounded below by a positive constant and $\mathbf{C}_\theta^n$ is uniformly bounded in $L^2(\Omega, \mathbb{R}^3)$, we deduce that $\mathbf{U}_\theta^n$ is uniformly bounded in $BV(\Omega, \mathbb{R}^3)$. Therefore there exists a couple $(\mathbf{U}, \mathbf{C}) \in BV(\Omega, \mathbb{R}^3) \times L^2(\Omega, \mathbb{R}^3)$ such that up to a subsequence

$\mathbf{U}_\theta^n \rightharpoonup \mathbf{U}_\theta$ weakly* in $BV(\Omega, \mathbb{R}^3)$,
$\mathbf{U}_\theta^n \to \mathbf{U}_\theta$ strongly in $L^1(\Omega, \mathbb{R}^3)$,
$\mathbf{C}_\theta^n \rightharpoonup \mathbf{C}_\theta$ weakly in $L^2(\Omega, \mathbb{R}^3)$.

By the lower semi-continuity of weighted total variation and L^2 norm, we obtain

$$\begin{aligned}F_\theta(\mathbf{U}_\theta, \mathbf{C}_\theta) &= \int_\Omega g|\nabla \mathbf{U}_\theta|dx + \frac{1}{2\theta}\int_\Omega |\mathbf{U}_\theta - \mathbf{C}_\theta|^2 dx + \frac{1}{2}\int_\Omega \hat{\lambda}|\mathbf{C}_\theta - \mathbf{C}_0|^2 dx \\ &\leqslant \liminf_{n\to\infty} \int_\Omega g|\nabla \mathbf{U}_\theta^n|dx + \frac{1}{2\theta}\int_\Omega |\mathbf{U}_\theta^n - \mathbf{C}_\theta^n|^2 dx \\ &\quad + \frac{1}{2}\int_\Omega \hat{\lambda}|\mathbf{C}_\theta^n - \mathbf{C}_0|^2 dx \\ &\leqslant \liminf_{n\to\infty} F_\theta^n(\mathbf{U}_\theta^n, \mathbf{C}_\theta^n).\end{aligned}$$

This implies that $(\mathbf{U}_\theta, \mathbf{C}_\theta)$ is a minimizer of the approximate problem (28).

We now pass the limit as $\theta \to 0^+$ and prove the convergence of the solution sequence $(\mathbf{U}_\theta, \mathbf{C}_\theta)$.

Theorem 6. *As $\theta \to 0^+$, the solution of the approximate problem (28) converges to the solution of the weighted TV colorization problem (27).*

Proof. Assume $(\mathbf{U}_\theta, \mathbf{C}_\theta)$ is a couple of solution to problem (28) for fixed $\theta \in (0,1)$ satisfying $|\mathbf{C}_\theta| = 1$, we have $F_\theta(\mathbf{U}_\theta, \mathbf{C}_\theta) \leqslant F_\theta(\mathbf{V}, \mathbf{W})$ for all $(\mathbf{V}, \mathbf{W}) \in BV(\Omega, \mathbb{R}^3) \times L^2(\Omega, \mathbb{R}^3)$, i.e.,

$$\begin{aligned}&\int_\Omega g|\nabla \mathbf{U}_\theta|dx + \frac{1}{2\theta}\int_\Omega |\mathbf{U}_\theta - \mathbf{C}_\theta|^2 dx + \frac{1}{2}\int_\Omega \hat{\lambda}|\mathbf{C}_\theta - \mathbf{C}_0|^2 dx \\ &\quad\leqslant \int_\Omega g|\nabla \mathbf{V}|dx + \frac{1}{2\theta}\int_\Omega |\mathbf{V} - \mathbf{W}|^2 dx + \frac{1}{2}\int_\Omega \hat{\lambda}|\mathbf{W} - \mathbf{C}_0|^2 dx.\end{aligned}$$

By taking $(\mathbf{V}, \mathbf{W}) \equiv (0,0)$, we obtain

$$\begin{aligned}&\int_\Omega g|\nabla \mathbf{U}_\theta|dx + \frac{1}{2\theta}\int_\Omega |\mathbf{U}_\theta - \mathbf{C}_\theta|^2 dx + \frac{1}{2}\int_\Omega \hat{\lambda}|\mathbf{C}_\theta - \mathbf{C}_0|^2 dx \\ &\quad\leqslant \frac{1}{2}\int_\Omega \hat{\lambda}\mathbf{C}_0^2 dx.\end{aligned}$$

Then there exists a constant M such that

$$\int_\Omega g|\nabla \mathbf{U}_\theta|dx \leqslant M,$$
$$\tfrac{1}{2}\int_\Omega |\mathbf{U}_\theta - \mathbf{C}_\theta|^2 dx \leqslant M\theta \leqslant M.$$

Thanks to g is bounded below by a positive constant and $|\mathbf{C}_\theta| = 1$, we conclude that $\mathbf{U}_\theta$ is uniformly bounded in $BV(\Omega, \mathbb{R}^3)$. Consider a sequence θ^n such that $\theta^n > 0$ and $\theta^n \to 0$ as $n \to \infty$. Then there exists $(\mathbf{U}, \mathbf{C}) \in BV(\Omega, \mathbb{R}^3) \times L^2(\Omega, \mathbb{R}^3)$ such that up to a subsequence,

$\mathbf{U}_{\theta^n} \rightharpoonup \mathbf{U}$ weakly* in $BV(\Omega)$,
$\mathbf{U}_{\theta^n} \to \mathbf{U}$ strongly in $L^1(\Omega)$,
$\mathbf{C}_{\theta^n} \rightharpoonup \mathbf{C}$ weaklyin $L^2(\Omega)$,
$\mathbf{U}_{\theta^n} - \mathbf{C}_{\theta^n} \to 0$ strongly in $L^2(\Omega)$.

Hence $\mathbf{U} = \mathbf{C}$ a.e. $x \in \Omega$. Thanks to the lower semi-continuity of vectorial TV and L^2 norm, we obtain for all $\mathbf{W} \in BV(\Omega)$ that

$$\begin{aligned}F(\mathbf{C}) &= \int_\Omega g|\nabla \mathbf{C}|dx + \frac{1}{2}\int_\Omega \hat{\lambda}|\mathbf{C} - \mathbf{C}_0|^2 dx \\ &\leqslant \liminf_{n\to\infty} \int_\Omega g|\nabla \mathbf{U}_{\theta^n}|dx + \frac{1}{2\theta^n}\int_\Omega |\mathbf{U}_{\theta^n} - \mathbf{C}_{\theta^n}|^2 dx \\ &\quad + \frac{1}{2}\int_\Omega \hat{\lambda}|\mathbf{C}_{\theta^n} - \mathbf{C}_0|^2 dx = \liminf_{n\to\infty} F_{\theta^n}(\mathbf{U}_{\theta^n}, \mathbf{C}_{\theta^n}) \\ &\leqslant \liminf_{n\to\infty} E_{\theta^n}(\mathbf{W}, \mathbf{W}) = \int_\Omega g|\nabla \mathbf{W}|dx \\ &\quad + \frac{1}{2}\int_\Omega \hat{\lambda}|\mathbf{W} - \mathbf{C}_0|^2 dx = F(\mathbf{W}).\end{aligned}$$

Thus $\mathbf{C}$ is a minimizer of F. □

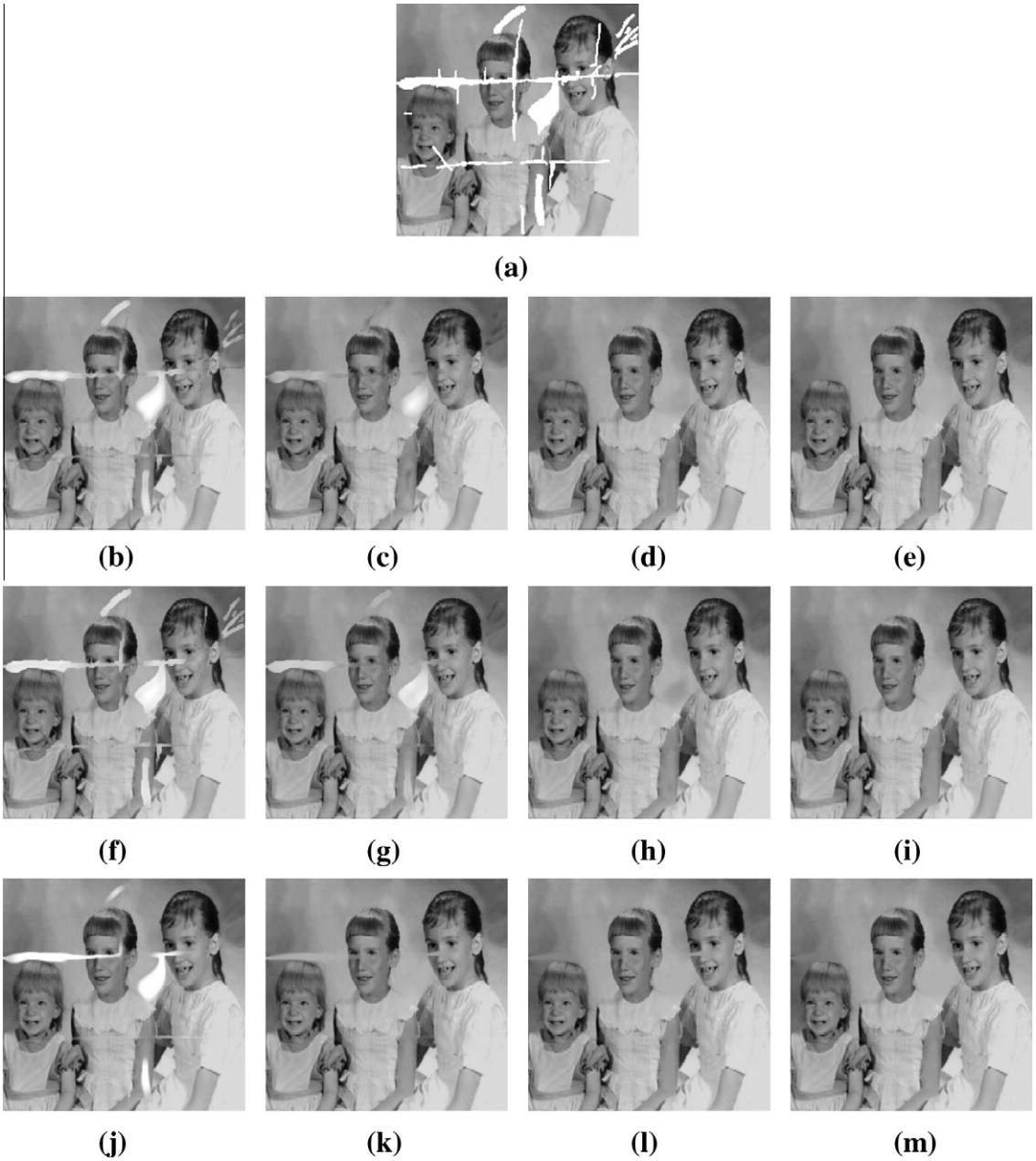

Fig. 1. Comparison of gray image inpainting algorithms. (a) The test image with inpainting mask (in white), size 256×256; results of the proposed algorithm I: (b)–(d) intermediate inpainting results at iterations 20, 40 and 120; (e) final inpainted image at iteration 200, computational time = 3.7 s; results of the split Bregman algorithm: (f)–(h) intermediate inpainting results at iterations 20, 40 and 120; (i) final inpainted image at iteration 200, computational time = 6.5 s; results of the implicit TV inpainting algorithm in [13]: (j)–(l) intermediate inpainting results at iteration 100, 1000 and 3000; (m) final inpainted image at iteration 5000, computational time = 87.4 s.

3.3. The algorithm

We use Lagrange multipliers method and relax the constraint in the approximate problem (28) as

$$\min_{\mu,\mathbf{U},\mathbf{C}} \int_\Omega g|\nabla \mathbf{U}|dx + \frac{1}{2\theta}\int_\Omega |\mathbf{U}-\mathbf{C}|^2 dx + \frac{1}{2}\int_\Omega \hat{\lambda}|\mathbf{C}-\mathbf{C}_0|^2 dx + \frac{1}{2}\int_\Omega \mu(|\mathbf{C}|^2-1)dx, \tag{30}$$

where $\mu(x)$ is the pointwise Lagrange multipliers. The above unconstrainted approximate problem can be decomposed into two subproblems:

$$\min_{\mathbf{U}} \int_\Omega g|\nabla \mathbf{U}|dx + \frac{1}{2\theta}\int_\Omega |\mathbf{U}-\mathbf{C}|^2 dx, \tag{31}$$

$$\min_{\mu,\mathbf{C}} \frac{1}{2\theta}\int_\Omega |\mathbf{U}-\mathbf{C}|^2 dx + \frac{1}{2}\int_\Omega \hat{\lambda}|\mathbf{C}-\mathbf{C}_0|^2 dx + \frac{1}{2}\int_\Omega \mu(|\mathbf{C}|^2-1)dx. \tag{32}$$

(31) can be solved by extending the dual vectorial ROF model of Bresson et al. [9] to weighted dual vectorial ROF model. The derivation of the formula is very easy and thus is omitted. See the formula in the details of algorithm III. Taking the derivative of energy in (32) with respect to $\mathbf{C}$ and setting the result to zero, we have

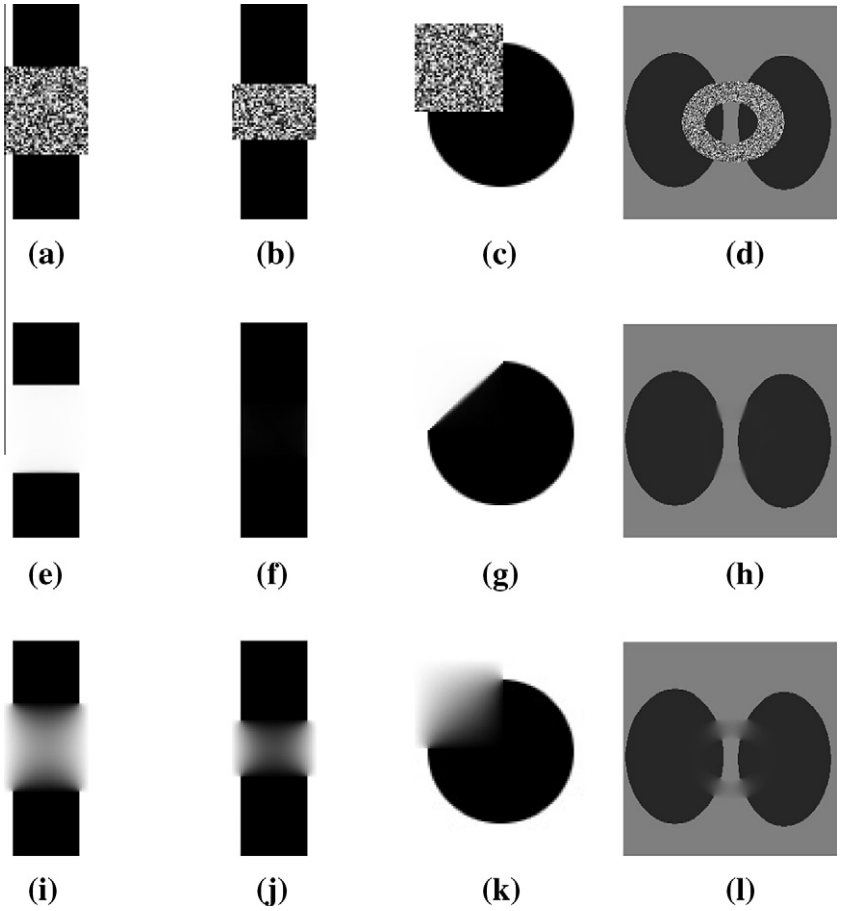

Fig. 2. Gray scale image inpainting by algorithm I and harmonic inpainting. The first row (a)–(d) are test images with inpainting mask filled in with random value, size of (a)–(c) 100×100, size of (d) 256×256; The second row (e)–(h) are the inpainting results by algorithm I; the third row (i)–(l) are the results of harmonic inpainting.

Fig. 3. Gray scale image inpainting by algorithm I. (a) Lena image with 30% information left, size 512×512; (b) inpainted image of (a) by algorithm I, PSNR = 31.8 dB: (c) Lena image with 10% information left; (d) inpainted image of (c) by algorithm I, PSNR = 25.9 dB. $\theta = 1$.

$$\frac{1}{\theta}(\mathbf{C}-\mathbf{U}) + \widehat{\lambda}(\mathbf{C}-\mathbf{C}_0) + \mu\mathbf{C} = 0. \tag{33}$$

Multiplying (33) by vector $\mathbf{C}$ and using the constraint $|\mathbf{C}| = 1$ yields

$$\mu(x) = \frac{1}{\theta}\langle \mathbf{U}, \mathbf{C}\rangle + \hat{\lambda}\langle \mathbf{C}, \mathbf{C}_0\rangle - \frac{1}{\theta} - \hat{\lambda}, \tag{34}$$

where $\langle \mathbf{U}(x), \mathbf{C}(x)\rangle = \sum_{i=1}^{3} \mathbf{U}_i(x)\mathbf{C}_i(x)$ denotes the inner product of vectors in $\mathbb{R}^3$. From (33) and (34), $\mathbf{C}$ is given by the following formula

$$\mathbf{C} = \frac{\mathbf{U} + \hat{\lambda}\theta\mathbf{C}_0}{1 + \hat{\lambda}\theta + \mu\theta}. \tag{35}$$

The algorithm details are as follows.

3.4. Algorithm III

- Initialization: $\mathbf{C}^0 = \mathbf{C}_0$, $\mathbf{p}^0 = \mathbf{0}$.
- Iteration: for $k = 0, 1, 2, \ldots$

$$\begin{aligned}
\mathbf{p}^{k+1} &= \frac{\mathbf{p}^k + \tau\nabla\left(\mathrm{div}\mathbf{p}^k - \mathbf{C}^k/\theta\right)/g}{1 + \tau\left|\nabla\left(\mathrm{div}\mathbf{p}^k - \mathbf{C}^k/\theta\right)\right|/g},\\
\mathbf{U}^{k+1} &= \mathbf{C}^k\theta\mathrm{div}\mathbf{p}^{k+1},\\
\mu^{k+1} &= \tfrac{1}{\theta}\langle \mathbf{U}^{k+1}, \mathbf{C}^k\rangle + \hat{\lambda}\langle \mathbf{C}^k, \mathbf{C}_0\rangle - \tfrac{1}{\theta} - \hat{\lambda},\\
\mathbf{C}^{k+1} &= \tfrac{\mathbf{U}^{k+1} + \hat{\lambda}\theta\mathbf{C}_0}{1 + \hat{\lambda}\theta + \mu^{k+1}\theta}.
\end{aligned}$$

- Termination criterion: as Algorithm I.

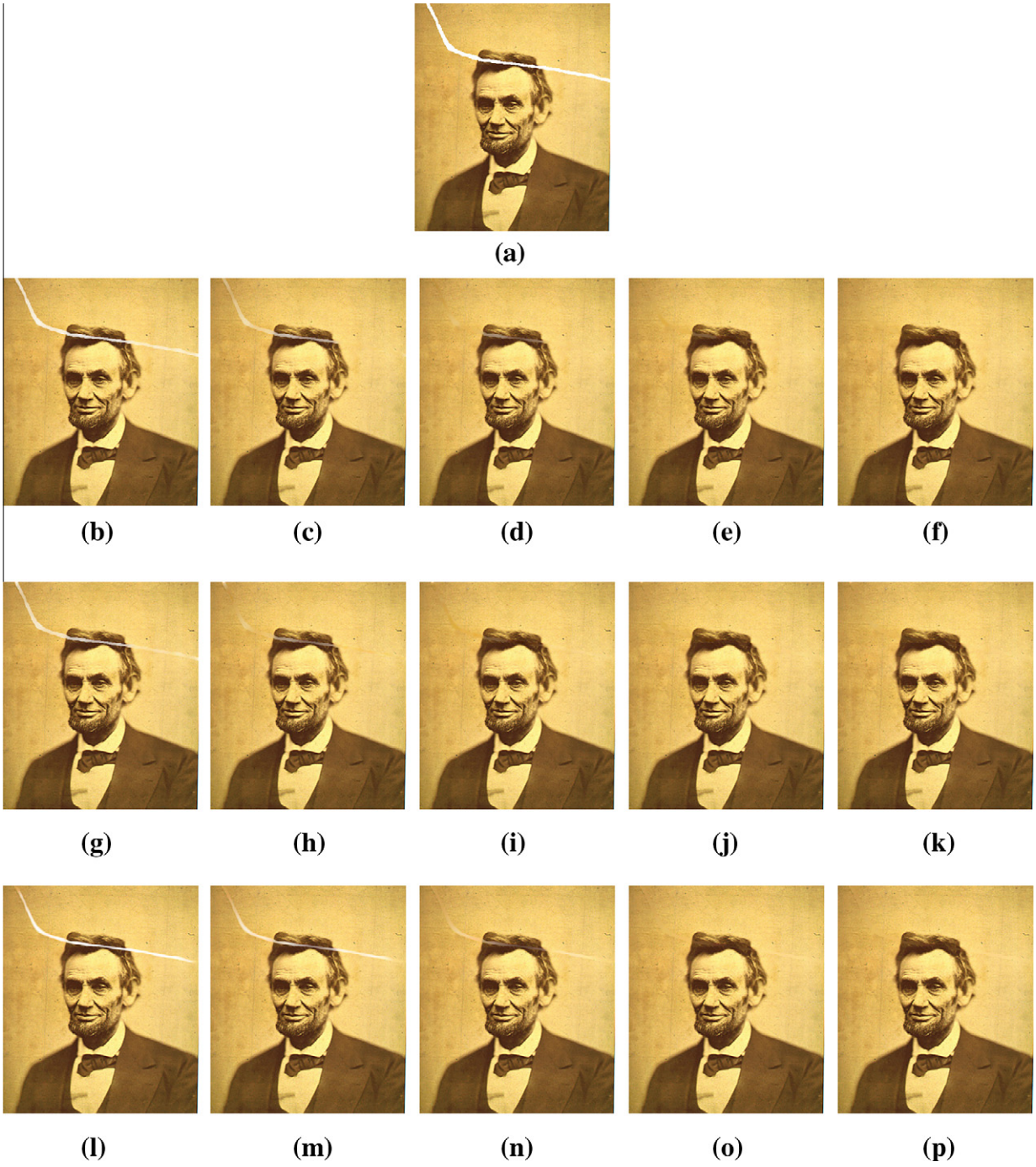

Fig. 4. Comparison of color image inpainting with algorithms. (a) The test image with mask, size 371 × 432; results of algorithm II: (b)–(e) intermediate inpainting results at iterations 20, 40, 60 and 100; (f) final inpainted image at iteration 100, computational time = 14.7 s; results of the SB algorithm: (g)–(j) intermediate inpainting results at iterations 20, 40, 60 and 100; (k) final inpainted image at iteration 100, computational time = 20.9 s; results of implicit algorithm as in [13] for model (3): (l)–(o) intermediate inpainting results at iteration 100, 200, 400 and 1000; (p) final inpainted image at iteration 1500, computational time = 141.3 s.

Compared with the method in [24], the advantages of our method are: (1) the Lagrange multipliers $\mu(x)$ can be automatically given by closed form solution in our method, while in [24], the Lagrange multiplier α should be defined by the user; (2) $\mathbf{C}$ has closed form solution in our method, while in [24], $\mathbf{C}$ is solved by implicit scheme or gradient descent method with small time step; (3) In [24], the chromaticity is projected to satisfy $|\mathbf{C}| \leqslant 1$ in each iteration in order to ensure the stability of the algorithm, which is not necessary in our algorithm.

4. Numerical results

We test our algorithms I, II and III on various images in this section. Default parameters are $\lambda = 10 * (1 - \chi_D)$, $\theta = 10$, $\tau = 0.125$ for algorithm I and II; $\lambda = 10 * (1 - \chi_D)$, $\theta = 0.05$, $\tau = 0.125$, $\sigma = 3$, $k = 0.05$ for algorithm III. We will note if other parameters are used. The experiments are performed under Windows XP and MATLAB v7.4 with Intel Core 2 Duo CPU at 1.66 GHz and 2 GB memory.

Some of the results are compared with other inpainting methods including the implicit TV inpainting algorithm in [13], the split Bregman (SB) algorithm in [21] and the harmonic inpainting method. The reason we choose these algorithms for comparison is that the algorithm in [13] and the harmonic inpainting are classical algorithms and the SB algorithm is one of the state of the art algorithm for TV restoration problems in the aspect of speed.

4.1. Test algorithm I

We test our algorithm I for gray scale image inpainting in Figs. 1–3. In Fig. 1, we show the intermediate results in the evolution process of algorithm I in the second row. The result Fig. 1(e) at iteration 200 consuming 3.7 s seems quite good. The results for SB algorithm are displayed in the third row. It gives the similar final result Fig. 1(i) at iteration 200 consuming 6.5 s. We also show the results of TV inpainting model [13] in the evolution process in the fourth row. The result Fig. 1(m) at iteration 5000 consuming 87.4 seconds is acceptable. Our algorithm I is obviously faster than the algorithm in [13] and is also faster than the SB algorithm.

In Fig. 2, four synthetic images are tested. Our results are better than the results of harmonic inpainting. The inpainting results of Figs. 2(a) and (b) by algorithm I are totally different: the bar is broken in Fig. 2(e) while the bar is connected in Fig. 2(f). Actually, if the height of inpainting mask h is larger than the width w of the black bar as in Fig. 2(a), the inpainting result is a broken bar as Fig. 2(e), while if $h < w$ as in Fig. 2(b), the inpainting result is a connected bar as Fig. 2(f). This phenomenon is also observed in [13], and the mathematical analysis is given there. Another drawback of algorithm I (also observed in TV inpainting model [13]) is that it can not remain curvature of isophote, see Fig. 2(g) for example.

In Fig. 3, we test our algorithm I using Lena image with 30% and 10% information left which is chosen randomly. The inpainted images by algorithm I are satisfactory.

4.2. Test algorithm II

We test our algorithm II for color image inpainting in Figs. 4–8. In Fig. 4, the intermediate results of both algorithm II, SB algorithm, and implicit algorithm as in [13] for color TV inpainting model (3) are displayed. To get the visually acceptable results in the last column, algorithm II takes 100 iterations and 14.7 s, SB algorithm takes 100 iterations and 20.9 s, meanwhile implicit algorithm takes 1500 iterations and 141.3 s. One region of the images are zoomed in for detailed comparison in Fig. 5. It shows that our result is slightly better than that of implicit algoritm for model (3) and similar to that of SB algorithm.

In Figs. 6–8, more color images are tested. Fig. 6(a) is a noisy image with mask. Fig. 6(b) show that our method can simultaneously denoise and inpaint the image. Figs. 7 and 8 show that our algorithm is effective in scratch removal and text removal.

4.3. Test algorithm III

We test our algorithm III for image colorization in Figs. 9–12. We compare algorithm III and the method in [24] (model (25)) in Fig. 9. The parameters for [24] are set as: time step $dt = 0.1$, $\alpha = 10$, $\lambda = 10*(1 - \chi_D)$. The recovered chromaticity by algorithm III (Fig. 9(e)) seems slightly better than that of method in [24] (Fig. 9(g)). To obtain the results, algorithm III needs 300 iteration and 5.8 seconds, while model (25) in [24] needs 15000 iterations and 170.2 s. It shows that algorithm III is much faster than method in [24]. Fig. 10 displays the colorization of an image with 50% color

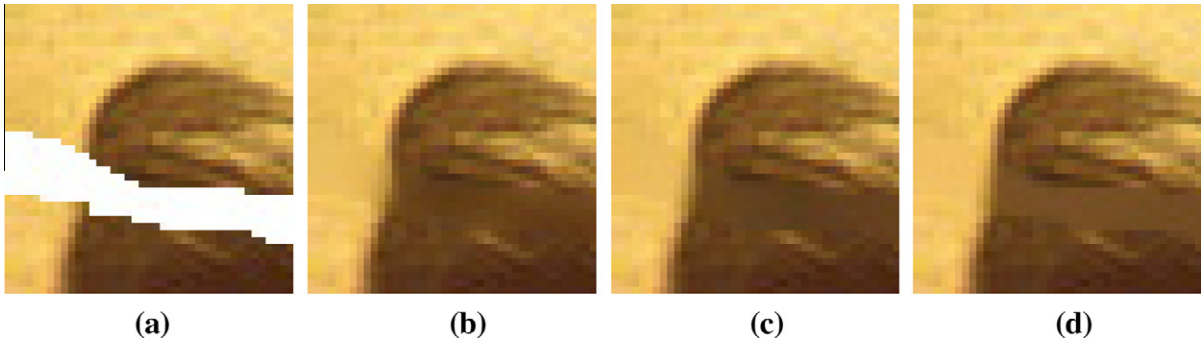

Fig. 5. Comparison of a small region in Fig. 4. (a) The test image; (b) inpainted by algorithm II; (c) inpainted by SB algorithm [21]; (d) inpainted by model (3).

Fig. 6. Color image denoising and inpainting by algorithm II. (a) Test image with mask which is contaminated by Gaussian noise with zero mean and standard deviation 20, size 384 × 256; (b) denoised and inpainted image by algorithm II. $\lambda = 0.05(1 - \chi_D)$.

Fig. 7. Scratch removal by algorithm II. (a) Test image with mask, size 600 × 406; (b) inpainted image.

Fig. 8. Text removal by algorithm II. (a) Test image with mask, size 800 × 600; (b) inpainted image.

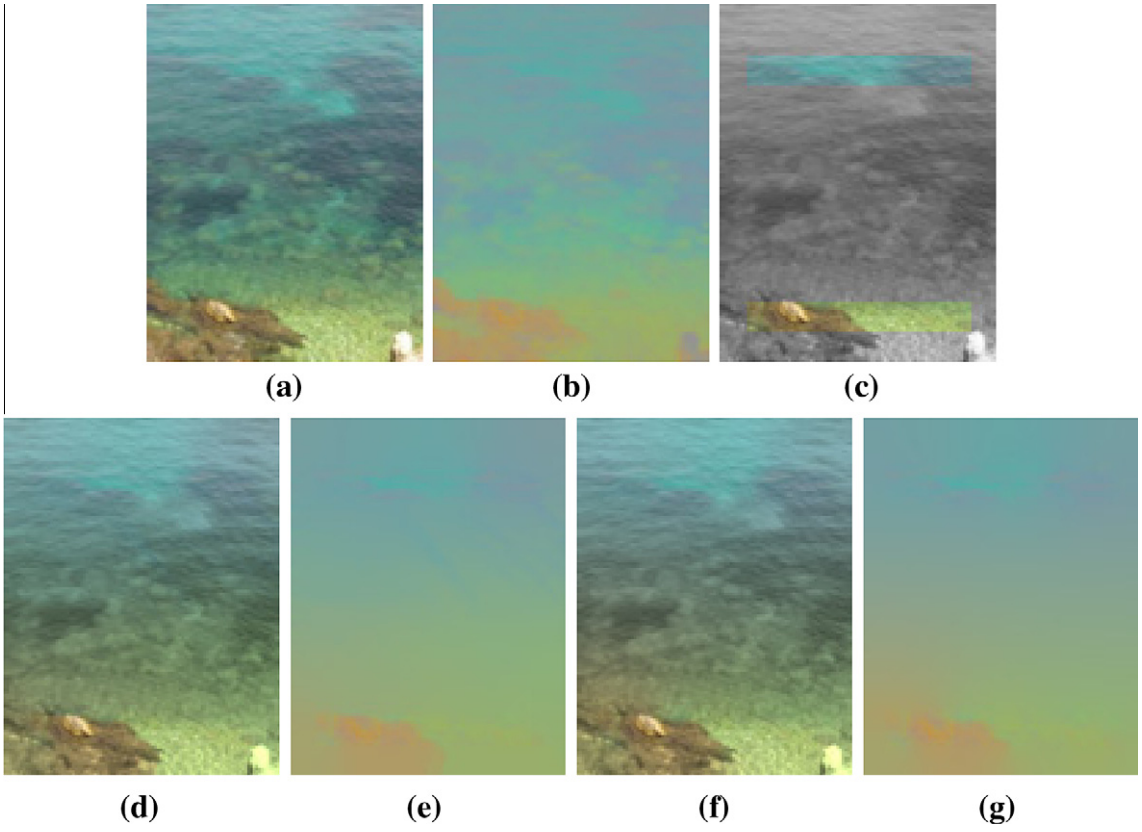

Fig. 9. Comparison of image colorization by algorithm III and method in [24]. (a) the original color image, size 101 × 131; (b) chromaticity of (a); (c) the color in the two strips are known; results of algorithm III: (d) the colorized image; (e) the recovered chromaticity, computational time = 5.8 s, iteration = 300; results of the method in [24]: (f) the colorized image; (g) the recovered chromaticity, computational time = 170.2 s, iteration = 15000.

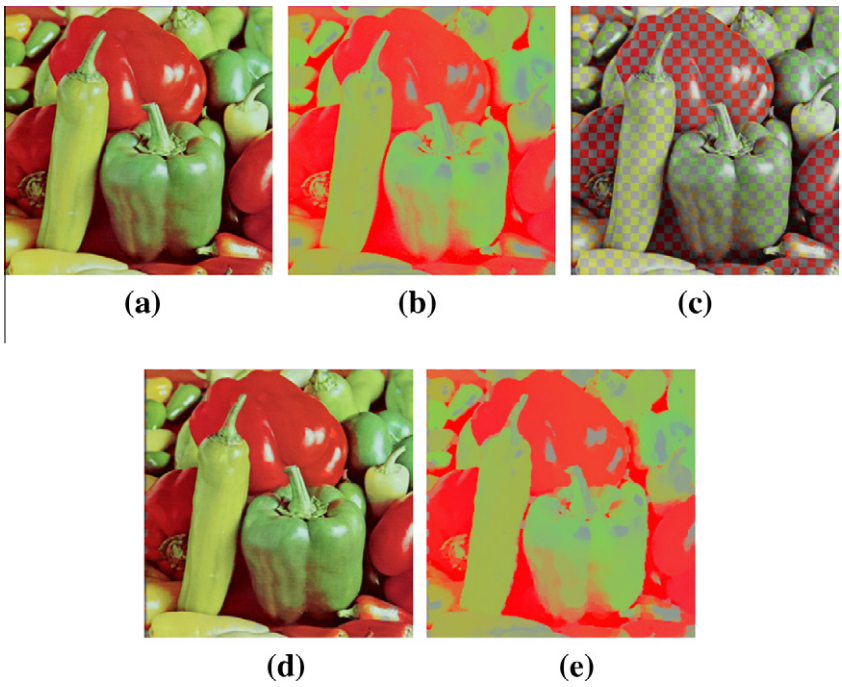

Fig. 10. Image colorization by algorithm III. (a) The original color image, size 256×256; (b) chromaticity of (a); (c) 50% color information are known (chessboard mask); results of algorithm III: (d) the colorized image; (e) the recovered chromaticity.

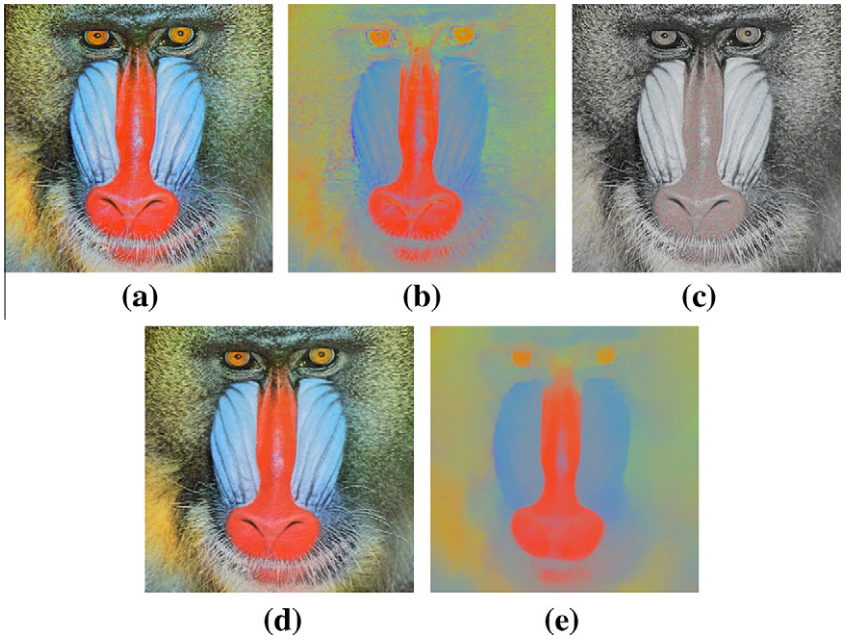

Fig. 11. Image colorization by algorithm III. (a) the original color image, size 512×512; (b) chromaticity of (a); (c) 10% color information are known (randomly chosen); results of algorithm III: (d) the colorized image; (e) the recovered chromaticity.

information left. Fig. 11 shows the colorization of an image with 10% color information left which is chosen randomly. The colorized images are very close to the original images. More images are colorized in Fig. 12 with given color in small regions. The results are satisfactory.

5. Conclusion

In this paper, we propose to approximate the TV inpainting model and TV colorization model by adding auxiliary variables in the original functionals such that the approximate problems can be solved by Chambolle's dual method and closed form solutions. The algorithms are far more efficient than the numerical schemes in [13,24] and competitive with the SB algorithm. Many mathematical results of the models are proved. We also observe in the experiments that our algorithm as well as TV inpainting has the drawback that it cannot remain the curvature of isophote. To overcome this drawback, geometric information such as curvature is introduced into the models in [14,17]. However, the numerical scheme is not efficient. In our future work, we plan to make use

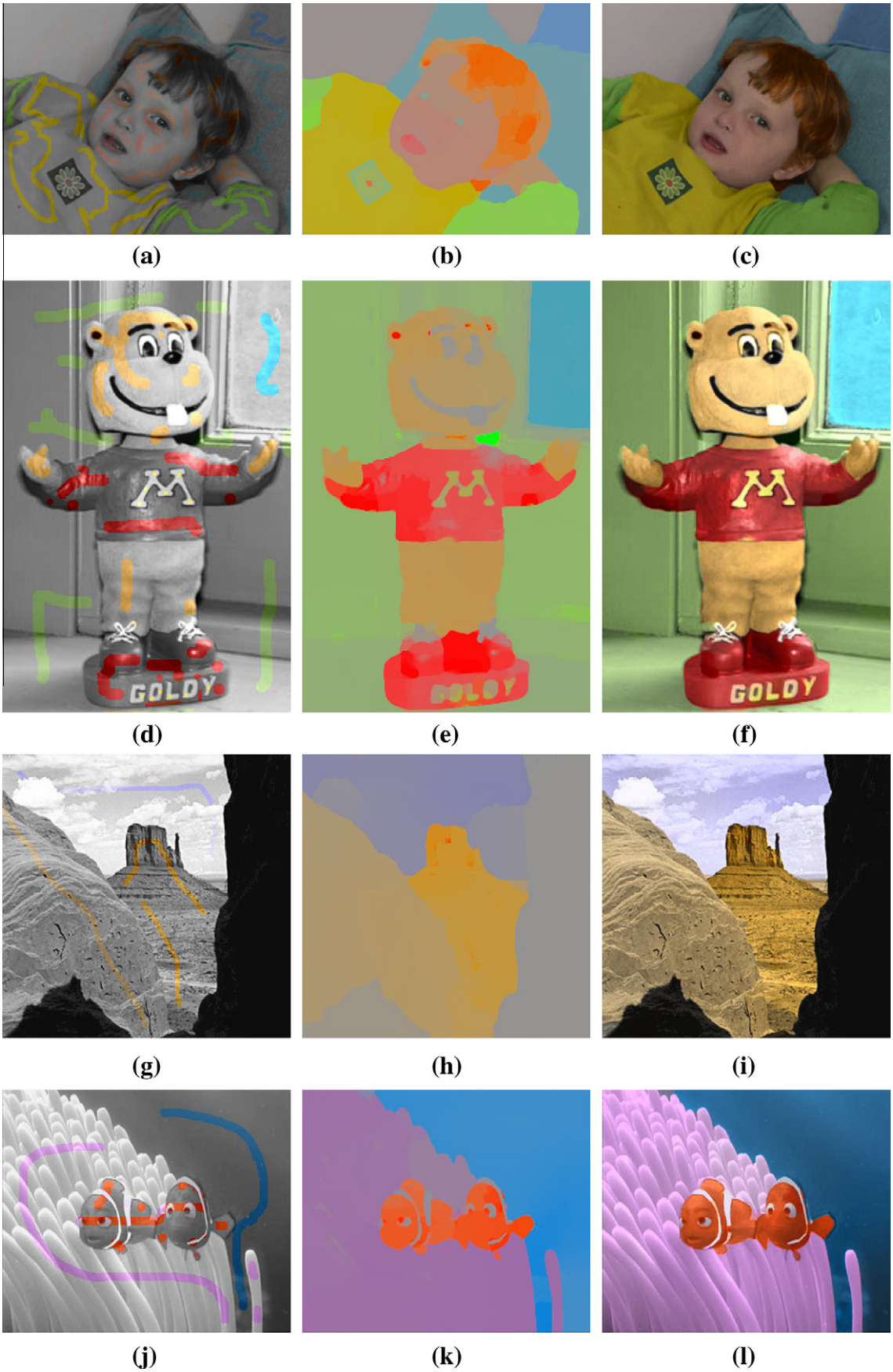

Fig. 12. Image colorization by algorithm III. First column: image with some known color; second column: the recovered chromaticity; third column: the colorized image.

of dual method to solve these models. Since higher order equation or functional are involved, the problem is more difficult.

Acknowledgements

The authors would like to thank the anonymous reviewers for their useful comments. This work is supported by the 973 Program (2011CB707104), the National Science Foundation of Shanghai (10ZR1410200), the National Science Foundation of China (11001082), the Chongqing CMEC foundation of China (KJ100818), and the CQUT foundation of China (2010ZQ13).

References

[1] F. Andreu-Vaillo, V. Caselles, J.M. Mazón, Parabolic Quasilinear Equations Minimizing Linear Growth Functionals, Birkhäuser, 2004.
[2] G. Aubert, P. Kornprobst, Mathematical Problems in Image Processing: Partial Differential Equations and the Calculus of Variations (Applied Mathematical Sciences), second ed., Springer-Verlag, 2006.
[3] C. Ballester, M. Bertalmo, V. Caselles, G. Sapiro, J. Verdera, Filling-in by joint interpolation of vector fields and gray levels, IEEE Trans. Image Process. 10 (2001) 1200–1211.
[4] A. Beck, M. Teboulle, Fast gradient-based algorithms for constrained total variation image denoising and deblurring problems, SIAM J. Imaging Sci. 2 (2009) 183–202.
[5] M. Bertalmio, G. Sapiro, V. Caselles, C. Balleste, Image inpainting, presented at the SIGGRAPH, New Orleans, LA, 2000.
[6] M. Bertalmo, A. Bertozzi, G. Sapiro, Navier–Stokes, fluid-dynamics and image and video inpainting, in: IEEE CVPR 2001, Hawaii, USA, December 2001.
[7] M. Bertalmio, L. Vese, G. Sapiro, S. Osher, Simultaneous structure and texture image inpainting, IEEE Trans. Image. Process. 12 (2003) 882–889.
[8] X. Bresson, S. Esedoglu, P. Vandergheynst, J.-P. Thiran, S. Osher, Fast Global Minimization of the Active Contour/Snake Model, J. Math. Imaging Vis 28 (2007) 151–167.
[9] X. Bresson, T.F. Chan, Fast minimization of the vectoral total variation norm and application to color image processing, UCLA CAM report 07-25.
[10] A. Chambolle, An algorithm for total variation minimization and applications, J. Math. Imaging Vis. 20 (2004) 89–97.
[11] J.-F. Cai, R.H. Chan, Z. Shen, A framelet-based image inpainting algorithm, Appl. Comput. Harmonic Anal. 24 (2008) 131–149.
[12] R.H. Chan, S. Setzer, G. Steidl, Inpainting by flexible Haar-wavelet shrinkage, SIAM J. Imaging Sci. 1 (2008) 273–293.
[13] T.F. Chan, J. Shen, Mathematical models for local nontexture inpaintings, SIAM J. Appl. Math. 62 (2002) 1019–1043. 200.
[14] T.F. Chan, J. Shen, Non-texture inpainting by curvature-driven diffusion (CDD), J. Vis. Comm. Image Represent 12 (2001) 436–449.
[15] T.F. Chan, S.H. Kang, Error analysis for image inpainting, J. Math. Imag. Vis. 26 (2006) 85–103.
[16] T.F. Chan, S.H. Kang, J. Shen, Total variation denoising and enhancement of color images based on the CB and HSV color models, J. Vis. Commun. Image Represent 12 (2001) 422–435.
[17] T.F. Chan, S.H. Kang, J. Shen, Eulers elastica and curvature based inpainting, SIAM J. Appl. Math. 63 (2002) 564–592.
[18] A. Criminisi, P. Perez, K. Toyama, Object Removal by Exemplar-Based Inpainting, CVPR, Madison, Wisconsin, 2003.
[19] E. Esser, Applications of Lagrangian-based alternating direction methods and connections to split Bregman, Technical report cam 09-31, UCLA Computational and Applied Mathematics, March 2009.
[20] L.C. Evans, R.F. Gariepy, Measure Theory and Fine Properties of Functions, Studies in Advanced Mathematics, CRC Press, Roca Baton, FL, 1992.
[21] T. Goldstein, S. Osher, The split Bregman method for L1 regularized problems, SIAM J. Imag. Sci. 2 (2) (2009) 323–343.
[22] H. Grossauer, A combined PDE and texture synthesis approach to inpainting, in: Proceedings of ECCV, 2004, LNCS 3022.
[23] H. Grossauer, O. Scherzer, Using the Complex Ginzburg–Landau Equation for Digital Inpainting in 2D and 3D, Scale-Space 2003, LNCS 2695, 2003, pp. 225–36.
[24] S.H. Kang, R. March, Variational models for image colorization via chromaticity and brightness decomposition, IEEE Trans. Image Process. 16 (2007) 2251–2261.
[25] A. Levin, D. Lischinski, Y. Weiss, Colorization using optimization, Proc. SIGGRAPH Conf. 23 (2004) 689–694.
[26] S. Masnou, J.-M. Morel, Level lines based disocclusion, in: Proc. Fifth IEEE Int. Conf. Image Process., Chicago, vol. 3, 1998, pp. 259–263.
[27] Y. Nesterov, Smooth minimization of non-smooth functions, Math. Program. 103 (2005) 127–152.
[28] K.A. Patwardhan, G. Sapiro, M. Bertalmio, Video inpainting of occluded and occluding objects, in: Proc. Int. Conf. Image Process. (ICIP), 2005.
[29] L. Rudin, S. Osher, E. Fatemi, Nonlinear total variation based noise removal algorithms, Phys. D. 60 (1992) 259–268.
[30] G. Sapiro, Inpainting the colors, Proc. IEEE Int. Conf. Image Process. 2 (2005) 698–701.
[31] S. Setzer. Operator splittings, Bregman methods and frame shrinkage in image processing, Int. J. Comput. Vis., doi:10.1007/s11263-010-0357-3.
[32] X.-C. Tai, S. Osher, R. Holm, Image Inpainting using a TV-Stokes Equation, In Image Processing Based on Partial Differential Equations, Springer, Heidelberg, 2006.
[33] L. Vese, S. Osher, Numerical methods for *p*-harmonic flows and applications to image processing, SIAM J. Numer. Anal. 40 (2002) 2085–2104.
[34] L. Yatziv, G. Sapiro, Fast image and video colorization using chrominance blending, IEEE Trans. Image Process. 15 (2006) 1120–1129.